
Ensemble Kalman Filter (EnKF) for Reinforcement Learning (RL)

Anant Joshi*

Coordinated Science Laboratory
University of Illinois at Urbana-Champaign
anantaj2@illinois.edu

Amirhossein Taghvaei

Department of Mechanical and Aerospace Engineering
University of California, Irvine
ataghvae@uci.edu

Prashant G. Mehta

Coordinated Science Laboratory
University of Illinois at Urbana-Champaign
mehtapg@illinois.edu

Abstract

This paper is concerned with the problem of representing and learning the optimal control law for the linear quadratic Gaussian (LQG) optimal control problem. In recent years, there is a growing interest in re-visiting this classical problem, in part due to the successes of reinforcement learning (RL). The main question of this body of research (and also of our paper) is to approximate the optimal control law *without* explicitly solving the Riccati equation. For this purpose, a novel simulation-based algorithm, namely an ensemble Kalman filter (EnKF), is introduced in this paper. The algorithm is used to obtain formulae for optimal control, expressed entirely in terms of the EnKF particles. For the general partially observed LQG problem, the proposed EnKF is combined with a standard EnKF (for the estimation problem) to obtain the optimal control input based on the use of the separation principle. A nonlinear extension of the algorithm is also discussed which clarifies the duality roots of the proposed EnKF. The theoretical results and algorithms are illustrated with numerical experiments.

1 Introduction

This paper is concerned with the problem of reinforcement learning (RL) in continuous-time and continuous (Euclidean) state-space settings. A special case is the linear quadratic Gaussian (LQG) problem where the dynamic model is a linear system, the cost terms are quadratic, and the distributions – of the random initial condition and the noise – are Gaussian.

The LQG problem has a rich and storied history in modern control theory going back to the very origin of the subject Kalman [1960]. To obtain the optimal control, the bottleneck is to solve the Riccati equation – the differential Riccati equation (DRE) in finite-horizon settings or the algebraic Riccati equation (ARE) in the infinite-horizon settings of the problem. There is a large body of

*

literature devoted to the analytical study of these equations Bittanti et al. [2012], Lancaster and Rodman [1995] and specialized numerical techniques have been developed to efficiently compute the solution Laub [1991], Benner and Bujanović [2016].

There are two issues which makes the LQG and related problems a topic of recent research interest: (i) In high-dimensions, the matrix-valued nature of the DRE or ARE means that any algorithm is $\mathcal{O}(d^2)$ in the dimension d of the state-space; and (ii) the model parameters may not be explicitly available to write down the DRE (or the ARE) let alone solve it. The latter is a concern, e.g., when the model exists only in the form of a black-box numerical simulator.

These two issues have motivated the recent research on the infinite-horizon linear quadratic regulator (LQR) problem Fazel et al. [2018], Tu and Recht [2019]. In LQR, the bottleneck is to solve an ARE. The algorithms studied in the recent papers seek to bypass solving an ARE by directly searching over the space of stabilizing gain matrices. Global convergence rate estimates are established for both discrete-time Fazel et al. [2018], Dean et al. [2020], Malik et al. [2020], Mohammadi et al. [2021] and continuous-time Mohammadi et al. [2020a,b, 2019] settings of the LQR problem. Extensions to the H_∞ regularized LQR Zhang et al. [2020] and Markov jump linear systems Jansch-Porto et al. [2020] have also been carried out.

The motivation and goals of the present work are related to these recent papers, albeit the proposed solution approach is very different. The inspiration for our work comes from the area of data assimilation (nonlinear filtering) Reich and Cotter [2015]. In most practical applications of data assimilation, e.g., in weather prediction, (i) only simulation-based models are available, and (ii) these are very high-dimensional. The ensemble Kalman filter (EnKF) is an efficient simulation-based algorithm to assimilate sensor data in these applications *without* the need to explicitly solve a DRE Evensen [1994, 2006], Houtekamer and Mitchell [2001].

The primary contribution of this work is to extend the EnKF algorithm to now solve the LQG optimal control problem. Specifically, a novel type of EnKF is proposed to approximate the optimal control law for the LQG problem. The proposed algorithm is simulated-based and, in particular, avoids the need to solve the DRE. Assuming full-state feedback, it directly yields the optimal control input. For the partially observed case, the proposed EnKF is combined with a standard EnKF (for the estimation problem) to obtain the optimal control input based on the use of the separation principle.

The second contribution of this paper is to extend these results to a class of nonlinear optimal control problems. A simulation-based algorithm is described to obtain the optimal control law without the need to explicitly solve the Hamilton-Jacobi-Bellman (HJB) equation. Instead, the proposed algorithm requires a solution of a linear Poisson equation. It is shown that the EnKF algorithm for the LQG problem is a special case where the Poisson equation admits an analytical solution.

The two contributions of this paper represent the optimal control counterparts of the EnKF Bergemann and Reich [2012b] and the feedback particle filter (FPF) Yang et al. [2013] algorithms that have been developed for the purposes of data assimilation Taghvaei et al. [2018].

The outline of the remainder of this paper is as follows. The LQG optimal control problem and its simulation-based solution is described in Sec. 2. Its nonlinear extension appears in Sec. 3. The algorithms are illustrated with numerical examples in Sec. 4.

Notation: $\mathcal{N}(m, \Sigma)$ is a Gaussian probability distribution with mean m and covariance Σ . The notation $\Sigma \succ 0$ is used when the matrix Σ is positive definite. For a smooth function $f : \mathbb{R}^d \rightarrow \mathbb{R}$, $\nabla f(x) = [\frac{\partial f}{\partial x_1}, \dots, \frac{\partial f}{\partial x_d}]^\top$ denotes the gradient of f , and $\nabla^2 f(x) = [\frac{\partial^2 f}{\partial x_m \partial x_n}(x)]_{n,m=1}^d$ denotes the Hessian matrix. For a smooth vector-field $v : \mathbb{R}^d \rightarrow \mathbb{R}^d$, $\nabla \cdot v(x) = \sum_{n=1}^d \frac{\partial v_n}{\partial x_n}(x)$ denotes the divergence. And for a smooth tensor $D : \mathbb{R}^d \rightarrow \mathbb{R}^{d \times d}$, $\nabla \cdot D(x)$ is a vector field whose m -th component is $\sum_{n=1}^d \frac{\partial D_{mn}}{\partial x_n}(x)$, and $\nabla^2 \cdot D(x) = \sum_{n,m=1}^d \frac{\partial^2 D_{mn}}{\partial x_n \partial x_m}(x)$.

2 Linear Quadratic Gaussian (LQG) problem

Problem: The partially observed linear Gaussian model is expressed using the Itô-stochastic differential equations (SDE) as

$$dX_t = AX_t dt + BU_t dt + d\xi_t, \quad X_0 \sim \mathcal{N}(m_0, \Sigma_0) \quad (1a)$$

$$dZ_t = HX_t dt + d\zeta_t, \quad Z_0 = 0 \quad (1b)$$

where $X = \{X_t \in \mathbb{R}^d : t \geq 0\}$ is the hidden state process, $U = \{U_t \in \mathbb{R}^m : t \geq 0\}$ is the control input, and $Z = \{Z_t \in \mathbb{R}^p : t \geq 0\}$ is the observation process. The model parameters A, B, H are matrices of appropriate dimensions, the process noise $\xi = \{\xi_t \in \mathbb{R}^d : t \geq 0\}$ and the observation noise $\zeta = \{\zeta_t \in \mathbb{R}^p : t \geq 0\}$ are Wiener processes (w.p.) with covariance Q and \mathcal{R} , respectively. It is assumed that X_0, ξ and ζ are mutually independent and $\mathcal{R} \succ 0$.

The LQG optimal control objective is to minimize

$$J(U) = \mathbb{E} \left(\int_0^T \frac{1}{2} |CX_t|^2 + \frac{1}{2} U_t^\top RU_t dt + \frac{1}{2} X_T^\top P_T X_T \right) \quad (2)$$

It is assumed that (A, B) is controllable, (A, C) and (A, H) are observable, and the matrices $P_T \succ 0$ and $R \succ 0$. In the fully observed settings, U_t is allowed to be a function of X_t . In the partially observed settings, U_t is a function of the past observations $\{Z_s : 0 \leq s \leq t\}$. For this purpose, it is convenient to denote $\mathcal{Z}_t := \sigma(\{Z_s : 0 \leq s \leq t\})$ as the sigma-field generated by the observations, and consider control inputs U which are adapted to the filtration $\mathcal{Z} := \{\mathcal{Z}_t : t \geq 0\}$.

Classical solution: Using the separation principle², the LQG controller is obtained in three steps:

Step 1. Filter design: The objective of the filter design step is to compute the causal estimate $\hat{X}_t := \mathbb{E}(X_t | \mathcal{Z}_t)$ for $t \geq 0$. The evolution equation for $\{\hat{X}_t : t \geq 0\}$ is the Kalman-Bucy filter. Notably, the optimal gain matrix for the filter is obtained by solving a forward (in time) DRE.

Step 2. Control design: The objective of the control design step is to compute the optimal feedback control law $\{u_t(x) : 0 \leq t \leq T, x \in \mathbb{R}^d\}$ for the fully observed LQG problem. It is well known to be of the linear form

$$u_t(x) = K_t x, \quad 0 \leq t \leq T$$

where the optimal gain matrix K_t is obtained by solving a backward (in time) DRE.

Step 3. Certainty equivalence: The optimal control input is obtained by combining the results from steps 1 and 2:

$$U_t = u_t(\hat{X}_t) = K_t \hat{X}_t, \quad 0 \leq t \leq T$$

The bottleneck is to solve the DREs – the forward DRE for the optimal filter gain and the backward DRE for the optimal control gain³. In the following three sections, we describe a simulation-based algorithm for these three steps which avoids the need to explicitly solve the DREs. The implementation details of the algorithm can be found in Appendix C.

2.1 Step 1. Filter design using EnKF

The filter design objective is to compute the causal estimate $\hat{X}_t = \mathbb{E}(X_t | \mathcal{Z}_t)$. In the linear Gaussian settings, the conditional distribution of the X_t is Gaussian whose mean and variance are denoted as m_t and Σ_t , respectively. These evolve according to the Kalman-Bucy filter:

$$dm_t = Am_t dt + BU_t dt + L_t(dZ_t - Hm_t dt), \quad m_0 = \mathbb{E}(X_0) \quad (3a)$$

$$\frac{d}{dt}\Sigma_t = A\Sigma_t + \Sigma_t A^\top + Q - \Sigma_t H^\top \mathcal{R}^{-1} H \Sigma_t, \quad \Sigma_0 = \text{var}(X_0) \quad (3b)$$

²The separation principle hinges on the assumption that the control input U_t does not change the observation sigma-field \mathcal{Z}_t . This is valid under very mild assumptions on the control policy, e.g. Lipschitz with respect to estimate \hat{X}_t . See [Van Handel, 2007, Sec. 7.3], Georgiou and Lindquist [2013] and references therein for a rigorous statement of allowed class of control policies.

³In the steady-state or infinite horizon settings (as $T \rightarrow \infty$), one may replace the optimal filter gain and the optimal control gain by their steady-state values. These are directly obtained by solving the respective AREs.

where $L_t = \Sigma_t H^\top \mathcal{R}^{-1}$ is the Kalman gain. Note that (3b) is a forward (in time) DRE and its solution Σ_t is used to compute the optimal Kalman gain L_t .

The EnKF is a simulation-based algorithm to approximate the Kalman filter, that does not require an explicit solution of the DRE (3b). The design of an EnKF proceeds in two steps:

1. Construct a stochastic process, denoted by $\bar{X} := \{\bar{X}_t \in \mathbb{R}^d : t \geq 0\}$, such that the conditional distribution (given \mathcal{Z}_t) of \bar{X}_t is equal to the conditional distribution of X_t ;
2. Simulate N stochastic processes, denoted by $\{X_t^i : t \geq 0, 1 \leq i \leq N\}$, to empirically approximate the distribution of \bar{X}_t .

The process \bar{X} is referred to as the mean-field process. The N processes in the step 2 are referred to as particles. The construction ensures that the EnKF is *exact* in the mean-field ($N = \infty$) limit. That is, for any bounded and continuous function f ,

$$\underbrace{\mathbb{E}[f(X_t)|\mathcal{Z}_t]}_{\text{exactness condition}} \xrightarrow{\text{Step 1}} \mathbb{E}[f(\bar{X}_t)|\mathcal{Z}_t] \xrightarrow{\text{Step 2}} \frac{1}{N} \sum_{i=1}^N f(X_t^i)$$

The details of the two steps are as follows:

Mean-field process: The mean-field process is constructed as

$$d\bar{X}_t = A\bar{X}_t dt + BU_t dt + d\bar{\xi}_t + \bar{L}_t (dZ_t - \frac{H\bar{X}_t + H\bar{m}_t}{2} dt), \quad \bar{X}_0 \sim \mathcal{N}(m_0, \Sigma_0) \quad (4)$$

where $\bar{\xi} := \{\bar{\xi}_t : t \geq 0\}$ is an independent copy of the process noise ξ , $\bar{L}_t := \bar{\Sigma}_t H^\top \mathcal{R}^{-1}$ is the Kalman gain and

$$\bar{m}_t := \mathbb{E}[\bar{X}_t|\mathcal{Z}_t], \quad \bar{\Sigma}_t := \mathbb{E}[(\bar{X}_t - \bar{m}_t)(\bar{X}_t - \bar{m}_t)^\top|\mathcal{Z}_t]$$

are the conditional mean and the conditional covariance, respectively, of \bar{X}_t . The right-hand side of (4) depends upon both the process (\bar{X}_t) as well as the statistics of the process ($\bar{m}_t, \bar{\Sigma}_t$). Such an SDE is an example of a McKean-Vlasov SDE. The proof of the following proposition is included in Appendix A (see also [Taghvaei and Mehta, 2020, Theorem 1]).

Proposition 1 (Exactness of EnKF). *Consider the mean-field EnKF (4) initialized with a Gaussian initial condition $\bar{X}_0 \sim \mathcal{N}(m_0, \Sigma_0)$. Suppose the control input U is a \mathcal{Z} -adapted stochastic process. Then its solution \bar{X}_t is a Gaussian random variable whose conditional mean and variance*

$$\bar{m}_t = m_t, \quad \bar{\Sigma}_t = \Sigma_t, \quad a.s., \quad t > 0$$

evolve the same as the Kalman filter (3).

Finite- N approximation: The mean-field process is simulated as an interacting particle system:

$$dX_t^i = \underbrace{AX_t^i dt + BU_t dt + d\xi_t^i}_{\text{i-th copy of model (1a)}} + \underbrace{L_t^{(N)} (dZ_t - \frac{HX_t^i + H\hat{X}_t^{(N)}}{2} dt)}_{\text{data assimilation step}}, \quad X_0^i \stackrel{\text{i.i.d.}}{\sim} \mathcal{N}(m_0, \Sigma_0) \quad (5)$$

where $\hat{X}_t^{(N)} := \frac{1}{N} \sum_{i=1}^N X_t^i$ is the empirical mean and

$$L_t^{(N)} = \frac{1}{N-1} \sum_{i=1}^N (X_t^i) (HX_t^i - H\hat{X}_t^{(N)})^\top \mathcal{R}^{-1} \quad (6)$$

is the empirical approximation of the optimal Kalman gain matrix. The system (5) is referred to as the square root form of the EnKF [Bergemann and Reich, 2012a, Eq (3.3)]. Note that the gain is approximated entirely in terms of particles *without* solving the DRE (3b).

The EnKF (5) is an example of a simulation-based algorithm in the sense that N copies of the model (1a) are simulated in parallel. The simulations are coupled through a term which is referred to as the data assimilation step. This term has a gain times error feedback control structure.

Remark 1. *The mean-field process (4) represents the mean-field limit of the finite- N system (5), as the number of particles $N \rightarrow \infty$. The convergence is justified based on the propagation of chaos Bishop and Del Moral [2018]. The computational complexity of an ENKF is $\mathcal{O}(Nd)$. EnKF is a workhorse in applications such as weather prediction where models are simulation-based Evensen [2006], Reich and Cotter [2015]. In these applications, the number of simulations $N \ll d$.*

2.2 Step 2. Control design using EnKF

This section contains the primary contribution of this paper. Assuming full-state feedback, the optimal control law for the LQG problem (1a)-(2) is

$$u_t(x) = K_t x \quad \text{where} \quad K_t = -R^{-1}B^\top P_t$$

is the optimal gain matrix and P_t is a solution of the backward (in time) DRE

$$-\frac{d}{dt}P_t = A^\top P_t + P_t A + C^\top C - P_t B R^{-1} B^\top P_t, \quad P_T \text{ (given)} \quad (7)$$

It is known that $P_t \succ 0$ for $0 \leq t \leq T$ whenever $P_T \succ 0$ [Brockett, 2015, Sec. 24]. Therefore, $S_t = P_t^{-1}$ is well-defined. It is straightforward to verify that S_t also solves a backward DRE

$$\frac{d}{dt}S_t = AS_t + S_t A^\top - BR^{-1}B^\top + S_t C^\top C S_t, \quad S_T = P_T^{-1}$$

The bottleneck is to solve the DRE (7). In the following, an EnKF is proposed to obtain a simulation-based approximation of the optimal control law u_t . As before, the construction proceeds in two steps: (i) definition of an exact mean-field process and (ii) its finite- N approximation.

Mean-field process: The objective is to construct a stochastic process, denoted $\bar{Y}_t \in \mathbb{R}^d$ at time t , whose variance equals P_t , the solution of the DRE (7). This is done by constructing $\bar{\mathcal{Y}} = \{\bar{\mathcal{Y}}_t \in \mathbb{R}^d : 0 \leq t \leq T\}$ as a solution of the following backward (in time) McKean-Vlasov SDE:

$$d\bar{\mathcal{Y}}_t = A\bar{\mathcal{Y}}_t dt + B d\bar{\eta}_t + \frac{1}{2} \bar{S}_t C^\top (C\bar{\mathcal{Y}}_t + C\bar{n}_t) dt, \quad \bar{\mathcal{Y}}_T \sim \mathcal{N}(0, S_T) \quad (8)$$

and defining

$$\bar{Y}_t := \bar{S}_t^{-1}(\bar{\mathcal{Y}}_t - \bar{n}_t)$$

where $\bar{\eta} = \{\bar{\eta}_t \in \mathbb{R}^m : t \geq 0\}$ is a w.p. with covariance matrix R^{-1} , $d\bar{\eta}$ in (8) denotes the backward Itô-integral [Nualart and Pardoux, 1988, Sec. 4.2], and

$$\bar{n}_t := \mathbb{E}[\bar{\mathcal{Y}}_t], \quad \bar{S}_t := \mathbb{E}[(\bar{\mathcal{Y}}_t - \bar{n}_t)(\bar{\mathcal{Y}}_t - \bar{n}_t)^\top]$$

The proof of the following proposition is included in Appendix B.

Proposition 2. *Consider the mean-field EnKF (8) initialized with a Gaussian initial condition $\bar{\mathcal{Y}}_T \sim \mathcal{N}(0, S_T)$. Then its solution $\bar{\mathcal{Y}}_t$ is a Gaussian random variable whose mean and variance*

$$\bar{n}_t = 0, \quad \bar{S}_t = S_t, \quad 0 \leq t \leq T$$

Consequently, \bar{Y}_t is also a Gaussian random variable with mean and variance

$$\mathbb{E}(\bar{Y}_t) = 0, \quad \mathbb{E}(\bar{Y}_t \bar{Y}_t^\top) = P_t, \quad 0 \leq t \leq T$$

and therefore (i) If the matrix B is explicitly known then the optimal gain matrix

$$K_t = -R^{-1}B^\top \mathbb{E}(\bar{Y}_t \bar{Y}_t^\top)$$

or else (when it is not) then (ii) define the Hamiltonian⁴ (or the Q -function) Mehta and Meyn [2009]

$$H(x, a, t) := \frac{1}{2}|Cx|^2 + \frac{1}{2}a^\top Ra + x^\top \mathbb{E}(\bar{Y}_t \bar{Y}_t^\top)(Ax + Ba)$$

from which the optimal control law is obtained as $u_t(x) = \arg \min_{a \in \mathbb{R}^m} H(x, a, t)$.

⁴The Hamiltonian $H(x, a, t)$ is in the form of an oracle because $(Ax + Ba)$ is the right-hand side of the simulation model (1a).

Finite- N approximation: The mean-field process is empirically approximated by simulating a system of interacting particles $\{\mathcal{Y}_t^i \in \mathbb{R}^d : 0 \leq t \leq T, i = 1, \dots, N\}$ according to

$$d\mathcal{Y}_t^i = \underbrace{A\mathcal{Y}_t^i dt + B d\eta_t^i}_{\text{i-th copy of model (1a)}} + \underbrace{S_t^{(N)} C^\top \left(\frac{C\mathcal{Y}_t^i + Cn_t^{(N)}}{2} \right) dt}_{\text{RL step}}, \quad \mathcal{Y}_T^i \stackrel{\text{i.i.d.}}{\sim} \mathcal{N}(0, P_T^{-1}) \quad (9)$$

$$Y_t^i = (S_t^{(N)})^{-1} (\mathcal{Y}_t^i - n_t^{(N)})$$

where η^i is a copy of $\bar{\eta}$, $n_t^{(N)} = N^{-1} \sum_{i=1}^N \mathcal{Y}_t^i$, and $S_t^{(N)} = \frac{1}{N-1} \sum_{i=1}^N (\mathcal{Y}_t^i - n_t^{(N)}) (\mathcal{Y}_t^i - n_t^{(N)})^\top$.

The EnKF (9) is an example of a simulation-based algorithm in the sense that N copies of the model (1a) are simulated in parallel. An intuitive explanation of each of the terms on the right-hand side of (9), and their relationship to standard RL approaches is as follows:

Representation: The unknown positive definite matrix P_t is encoded in terms of statistics (variance) of the particles. Such a representation is fundamentally distinct from representing the value function, or its proxies, such as the Q function, in terms of a set of basis functions Devraj et al. [2020], Maei et al. [2010], Fujimoto et al. [2018], Melo et al. [2008].

Dynamics: The first term “ $A\mathcal{Y}_t^i dt$ ” on the right-hand side of (9) is simply a copy of uncontrolled dynamics in the model (1a).

Control: The second term is the control input “ $BU_t dt$ ” implemented as “ $B d\eta_t^i$ ”. That is, the control input U for the i -th particle is a white noise process with covariance R^{-1} . One may interpret this as an exploration step whereby the cheaper control directions are explored more.

In summary, for the i -th particle, the dynamics and control are the same as any RL algorithm (white noise is used for exploration). The difference arises due to the third term.

RL step: The third term indicated as the RL step engenders a particle flow that effectively implements the value iteration step of the RL. There are several points to be made:

1. The RL step is a function of the state cost term in (2). This is most easily seen by writing the equation for the empirical mean

$$dn_t^{(N)} = (A + S_t^{(N)} C^\top C) n_t^{(N)} dt + B d\eta_t^{(N)}, \quad n_T^{(N)} = 0$$

where $\eta_t^{(N)} = N^{-1} \sum_i \eta_t^i$. Noting that the state cost term is $x^\top C^\top C x$, the RL step implements a gradient with $S_t^{(N)} C^\top$ as the gain matrix.

2. The RL step has a linear feedback control structure and serves to couple the particles. Without the RL step, the particles are independent of each other.
3. This form of the RL step is possible *only* if one has access to a simulator and an ability to add additional terms outside the control channel (same as the data assimilation step in estimation). For example, this is not possible when the system exists only as an experiment.

It remains to use the finite- N system to approximate the optimal control law.

Optimal control: There are two cases to consider: (i) If the matrix B is explicitly known then⁵

$$K_t^{(N)} = -\frac{1}{N-1} \sum_{i=1}^N R^{-1} (B^\top Y_t^i) (Y_t^i)^\top \quad (10)$$

or else (when it is not) then (ii) approximate the Hamiltonian as

$$H^{(N)}(x, a, t) := \frac{1}{2} |Cx|^2 + \frac{1}{2} a^\top Ra + \frac{1}{N-1} \sum_{i=1}^N (x^\top Y_t^i) (Y_t^i)^\top \underbrace{(Ax + Ba)}_{\text{model (1a)}}$$

from which the optimal control law is obtained as

$$u_t^{(N)}(x) = \arg \min_{a \in \mathbb{R}^m} H^{(N)}(x, a, t)$$

⁵Eq. (10) for the optimal control gain matrix $K_t^{(N)}$ is dual to the eq. (6) for optimal filter gain matrix $L_t^{(N)}$.

There are several zeroth-order approaches to solve the minimization problem, e.g., by constructing 2-point estimators for the gradient. Since the objective function is quadratic and the matrix R is known, m queries of $H^{(N)}(x, \cdot, t)$ are sufficient to compute $u_t^{(N)}(x)$. This procedure is compared to the model-free policy optimization based methods for the LQR problem Mohammadi et al. [2021]. In policy optimization, the value $J(U)$ is minimized over the search space of stabilizing gain matrices, using a gradient descent approach. For each perturbation of the gain matrix, the gradient is estimated by simulating N trajectories over a time-horizon T . In contrast, using the EnKF, the matrix P_t is estimated by simulating N trajectories (simulation of EnKF is an offline calculation). Then the optimal control is obtained from an application of the minimum principle that only requires m evaluations at each t (the minimization of Hamiltonian is an online calculation).

2.3 EnKF-based algorithm for the LQG controller

By combining the result of steps 1 and 2, the optimal control input

$$U_t = \begin{cases} K_t^{(N)} \hat{X}_t^{(N)} & \text{if } B \text{ is known} \\ u_t^{(N)}(\hat{X}_t^{(N)}) & \text{o.w.} \end{cases}$$

The overall algorithm including steps 1, 2 and 3 is tabulated in the supplementary material where additional remarks on numerical approximation of backward SDEs and the error analysis (as the number of particles $N \rightarrow \infty$ and discretization time-step $\delta t \rightarrow 0$) also appear.

3 A nonlinear extension

Consider the nonlinear optimal control problem:

$$\begin{aligned} \min_U \quad J(U) &= \mathbb{E} \left(\int_0^T \left(\frac{1}{2} |c(X_t)|^2 + \frac{1}{2} U_t^\top R U_t \right) dt + g(X_T) \right) \\ \text{subject to:} \quad dX_t &= a(X_t) dt + b(X_t) U_t dt + \sigma(X_t) d\xi_t \end{aligned}$$

where X is the state, U is the control, and the process noise ξ is a standard w.p. (as before). The vector fields $a(\cdot)$, $b(\cdot)$, $c(\cdot)$, $g(\cdot)$, and $\sigma(\cdot)$ are continuously differentiable functions of their arguments and the control penalty parameter $R \succ 0$. For the calculations described next, it is useful to define two diffusion tensors $Q(x) := \sigma(x)\sigma^\top(x)$ and $D(x) := b(x)R^{-1}b^\top(x)$.

The solution is easily obtained using a standard dynamic programming (DP) argument.

Dynamic programming: For $t \in (0, T)$, the value function

$$v_t(x) := \min_{\{U_s: t \leq s \leq T\}} \mathbb{E} \left(\int_t^T \left(\frac{1}{2} |c(X_s)|^2 + \frac{1}{2} U_s^\top R U_s \right) ds + g(X_T) \middle| X_t = x \right) \quad (11)$$

From the DP optimality principle, the value function solves the HJB equation

$$\frac{\partial v_t}{\partial t} + \frac{1}{2} c^2 - \frac{1}{2} \nabla v_t^\top D \nabla v_t + a^\top \nabla v_t + \frac{1}{2} \text{Tr}(Q \nabla^2 v_t) = 0, \quad v_T = g \quad (12)$$

and the optimal control input is of the state feedback form $U_t = u_t(X_t)$ where

$$u_t(x) = -R^{-1}b^\top(x) \nabla v_t(x) \quad (13)$$

is the optimal control law. For the LQG special case, the value function $v_t(x) = \frac{1}{2}x^\top P_t x + (\text{constant})$ is quadratic and the HJB equation reduces to the DRE for the matrix P_t .

Solving the HJB equation is the bottleneck in obtaining the optimal control law. In the following, a mean-field process is introduced based on the use of a log transformation.

Log transformation: Defined the probability density $p_t(x) \propto e^{-v_t(x)}$. As part of the supplementary material, it is shown that the density evolves according to a backward equation

$$\frac{\partial p_t}{\partial t} = -\nabla \cdot (p_t a) + p_t (h_t - \hat{h}_t) + \nabla \cdot (p_t \nabla \cdot D) - \frac{1}{2} \nabla^2 \cdot (p_t D), \quad p_T \propto e^{-g} \quad (14)$$

where

$$h_t = \frac{1}{2}c^2 + \nabla \cdot a - \frac{1}{2}\nabla^2 \cdot D + \frac{1}{2}\text{Tr}((D - Q)\nabla^2 \log(p_t))$$

and $\hat{h}_t := \int h_t(x)p_t(x) dx$.

Mean-field process: A mean-field process $\bar{\mathcal{Y}} = \{\bar{\mathcal{Y}}_t \in \mathbb{R}^d : 0 \leq t \leq T\}$ is defined as follows:

$$d\bar{\mathcal{Y}}_t = a(\bar{\mathcal{Y}}_t) dt + b(\bar{\mathcal{Y}}_t) d\bar{\eta}_t + \nabla \cdot D(\bar{\mathcal{Y}}_t) dt + \mathcal{V}_t(\bar{\mathcal{Y}}_t) dt, \quad \bar{\mathcal{Y}}_T \sim p_T \quad (15)$$

where $\bar{\eta} := \{\bar{\eta}_t \in \mathbb{R}^m : 0 \leq t \leq T\}$ is a w.p. with covariance R^{-1} , and $\mathcal{V}_t(\cdot)$ is a vector-field that solves the first order linear partial differential equation (PDE)

$$-\frac{1}{\bar{p}_t(x)}\nabla \cdot (\bar{p}_t(x)\mathcal{V}_t(x)) = (h_t(x) - \hat{h}_t), \quad \forall x \in \mathbb{R}^d \quad (16)$$

where $\hat{h}_t := \int h_t(x)\bar{p}_t(x) dx$ and \bar{p}_t is the density of $\bar{\mathcal{Y}}_t$ at time t .

The following proposition relates the density $\bar{p}_t(x)$ of the mean-field process and the value function $v_t(x)$ of the optimal control problem. The relationship is useful to obtain an expression for the optimal control law. Its proof appears in Appendix D.

Proposition 3. Suppose $p_t \propto e^{-v_t}$ and \bar{p}_t is the density $\bar{\mathcal{Y}}_t$ at time t . Then provided $p_T = \bar{p}_T$,

$$p_t(x) = \bar{p}_t(x), \quad \forall x \in \mathbb{R}^d, 0 \leq t \leq T$$

Consequently, the optimal control law is given by

$$u_t(x) = R^{-1}b^\top(x)\nabla \log \bar{p}_t(x)$$

A finite N algorithm to implement the control law described in this section is presented in Appendix E.

Example 1. In the LQG example, $a(x) = Ax$ and $c(x) = Cx$ are linear vector-valued functions, $b(x) = B$ and $\sigma = Q^{\frac{1}{2}}$ are constant matrices, and p_t is Gaussian. In this case, $\nabla \cdot D = 0$ and the function $h_t(x)$ simplifies considerably because

$$\nabla \cdot a(x) = (\text{constant}), \quad \nabla^2 \cdot D = 0, \quad \text{Tr}((D - Q)\nabla^2 \log(p_t(x))) = (\text{constant})$$

Therefore, the right-hand side of the PDE (16) is given by

$$h_t(x) - \hat{h}_t = \frac{1}{2}|Cx|^2 - \frac{1}{2}\text{Tr}(C^\top C(\bar{S}_t + \bar{n}_t\bar{n}_t^\top))$$

It is straightforward to verify that

$$\mathcal{V}_t(x) = \frac{1}{2}S_t C^\top C(x + \bar{n}_t)$$

solves the PDE (16). Therefore, for LQG, the equation for $\bar{\mathcal{Y}}$ reduces to the form described in (8).

Remark 2. The first order PDE (16) is well known to arise in the nonlinear data assimilation literature Pathiraja et al. [2020], Daum et al. [2017], Crisan and Xiong [2010]. One of the issues with the PDE is that its solution is not unique. For this reason, it is useful to consider the gradient form solution such that $\mathcal{V}_t(x) = \nabla \phi_t(x)$. The resulting PDE

$$-\frac{1}{\bar{p}_t(x)}\nabla \cdot (\bar{p}_t(x)\nabla \phi_t(x)) = h_t(x) - \hat{h}_t$$

is referred to as the Poisson equation where the operator on the left-hand side is the weighted Laplacian. There is a well developed theory for existence and uniqueness of the solution of the Poisson equation (based upon assuming a suitable Poincaré inequality). Numerical algorithms have also been developed for its numerical approximation using particles Taghvaei et al. [2020].

Remark 3. In solving the first order PDE (16) or the Poisson equation, an additional difficulty arises here on account of approximating the right-hand side, the function $(h_t(x) - \hat{h}_t)$. In applications, some of these terms may be zero as noted below:

1. The term $\nabla \cdot a(x) = 0$ for conservative systems.
2. The term $\frac{1}{2} \text{Tr}((D(x) - Q(x)) \nabla^2 \log(p_t(x)))$ is zero whenever $b(x) = \sigma(x)$.
3. The term $\nabla^2 \cdot D(x) = 0$ if $b(x) = B$, a constant matrix.

Even if these are not zero, $h_t(x) \approx \frac{1}{2}|c(x)|^2$ (the state cost) is a useful approximation. Combined with the calculations in the Example 1, a finite- N algorithm is then obtained based on the Gaussian approximation of the density. The algorithm appears as part of the supplementary material.

Remark 4. The log transformation has a long history both in nonlinear filtering Fleming and Mitter [1982] and in optimal control Fleming [1977]. The transformation is an expression of the duality between optimal control and optimal estimation Mitter and Newton [2003], Todorov [2008]. Therefore, it has both been used to:

- (i) Obtain linearly solvable sampling algorithms to solve optimal control problems Kappen and Ruiz [2016], Rawlik et al. [2013], Theodorou et al. [2010], Schütte et al. [2012], Todorov [2009]; and
- (ii) Set up optimal control problems for the purposes of estimation and simulation Sutter et al. [2016], Hartmann and Schütte [2012], Van Handel [2006], Kim and Mehta [2020].

Although novel and distinct from the algorithms described in these earlier works – which instead rely on the use of a Feynman-Kac representation – the mean-field process (15)-(16) is an example of the sampling algorithm to solve the optimal control problem. The EnKF algorithm arises as a special case in the LQG settings of the problem. Given the enormous success of EnKF in data assimilation, the contributions of this paper potentially open up new opportunities for RL.

4 Numerics

1. Coupled mass spring damper system: The first example is the LQR problem for a linear mass spring damper system from Mohammadi et al. [2019]. For each mass, there are two states, position and velocity. A system with $\frac{d}{2}$ masses is d -dimensional. The finite- N algorithm is used to obtain an empirical approximation $\{P_t^{(N)} \in \mathbb{R}^{d \times d} : 0 \leq t \leq T\}$. The exact $\{P_t \in \mathbb{R}^{d \times d} : 0 \leq t \leq T\}$ is obtained by directly solving the backward DRE. The two are compared using the

$$\text{MSE} := \frac{1}{T} \mathbb{E} \left(\int_0^T \frac{\|P_t - P_t^{(N)}\|_F^2}{\|P_t\|_F^2} dt \right)$$

where $\|\cdot\|_F$ is the Frobenius (matrix) norm. The MSE is approximated empirically by averaging the integral over 100 simulation runs. See Appendix F.1 for details on modeling, parameter values, and the numerical discretization.

Figure 1 depicts the results of the numerical experiments showing the $O(\frac{1}{N})$ decay of MSE as the number of particles N increases (for each fixed d).

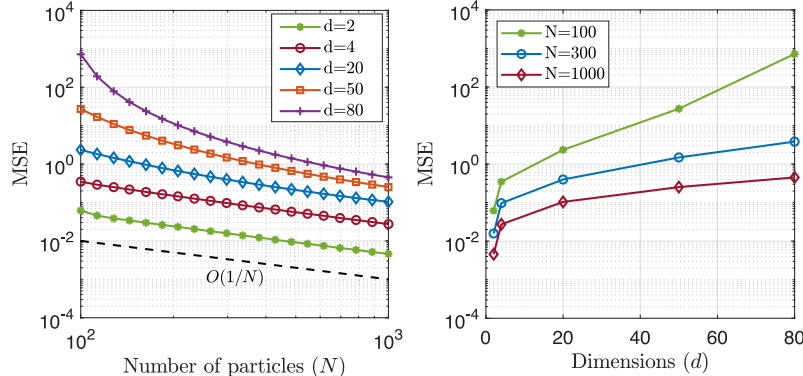


Figure 1: MSE for the mass springer damper system.

2. Cart pole system: The second example is the nonlinear conservative cart pole model Tedrake, Rawlik et al. [2013]. The control acts as external force applied to the cart. The four-dimensional state for the system is (θ, x, ω, v) , where $\theta \in S^1$ (the circle) is the angle of the pole (pendulum) as measured from the stable equilibrium, $x \in \mathbb{R}$ is the displacement of cart along the horizontal, and $(\omega, v) := (\dot{\theta}, \dot{x}) \in \mathbb{R}^2$ is the velocity vector. The control objective is to balance the pole – stabilize the system at the inverted equilibrium $(\pi, 0, 0, 0)$, assuming full state feedback. For the purposes of control design, the nonlinear system is first linearized at the desired equilibrium and an LQR problem is formulated (see Appendix F.2 for details). For the purposes of evaluation, the optimal control is applied to the full nonlinear model.

Figure 2 depict the results of numerical experiments for three different choices of N . It is seen that as few as $N = 10$ particles are sufficient to stabilize the equilibrium. Using $N = 1000$ particles, the closed-loop trajectories are virtually indistinguishable from the DRE-based solution.

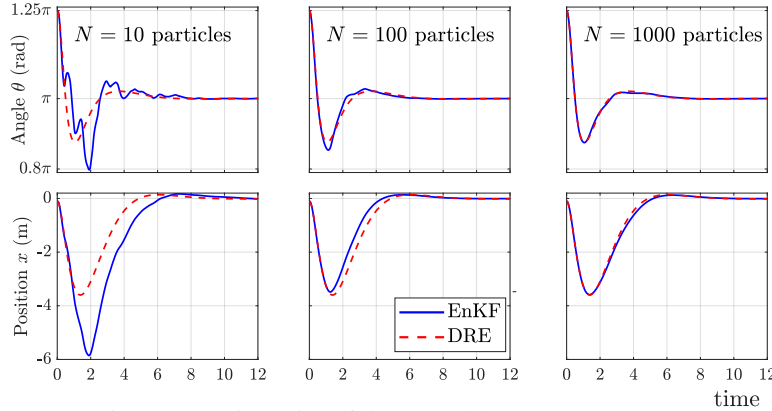


Figure 2: Trajectories of the closed-loop cart pole system.

References

P. Benner and Z. Bujanović. On the solution of large-scale algebraic Riccati equations by using low-dimensional invariant subspaces. *Linear Algebra and its Applications*, 488:430–459, 2016.

K. Bergemann and S. Reich. An ensemble Kalman-Bucy filter for continuous data assimilation. *Meteorologische Zeitschrift*, 21(3):213–219, 2012a. doi: 10.1127/0941-2948/2012/0307.

K. Bergemann and S. Reich. An ensemble Kalman-Bucy filter for continuous data assimilation. *Meteorologische Zeitschrift*, 21(3):213, 2012b.

A. N. Bishop and P. Del Moral. On the stability of matrix-valued Riccati diffusions. *arXiv preprint arXiv:1808.00235*, 2018. URL <https://arxiv.org/abs/1808.00235>.

A. N. Bishop, P. Del Moral, K. Kamatani, B. Remillard, et al. On one-dimensional riccati diffusions. *Annals of Applied Probability*, 29(2):1127–1187, 2019.

Sergio Bittanti, Alan J Laub, and Jan C Willems. *The Riccati Equation*. Springer Science & Business Media, 2012.

R. W Brockett. *Finite dimensional linear systems*. SIAM, 2015.

D. Crisan and J. Xiong. Approximate McKean-Vlasov representations for a class of SPDEs. *Stochastics*, 82(1):53–68, 2010. doi: 10.1080/17442500902723575.

F. Daum, J. Huang, and A. Noushin. Generalized Gromov method for stochastic particle flow filters. In *SPIE Defense+ Security*, pages 102000I–102000I. International Society for Optics and Photonics, 2017. doi: 10.1117/12.2248723.

S. Dean, H. Mania, N. Matni, B. Recht, and S. Tu. On the Sample Complexity of the Linear Quadratic Regulator. *Found Comput Math*, 20(4):633–679, August 2020. ISSN 1615-3383. doi: 10.1007/s10208-019-09426-y. URL <https://doi.org/10.1007/s10208-019-09426-y>.

P. Del Moral and J. Tugaut. On the stability and the uniform propagation of chaos properties of ensemble Kalman–Bucy filters. *Ann. Appl. Probab.*, 28(2):790–850, 04 2018. doi: 10.1214/17-AAP1317. URL <https://doi.org/10.1214/17-AAP1317>.

A. M. Devraj, A. Busic, and S. Meyn. Fundamental design principles for reinforcement learning algorithms. In K. G. Vamvoudakis, Y. Wan, F. L. Lewis, and D. Cansever, editors, *Handbook on Reinforcement Learning and Control*. Springer, 2020.

G. Evensen. Sequential data assimilation with a nonlinear quasi-geostrophic model using Monte Carlo methods to forecast error statistics. *Journal of Geophysical Research: Oceans*, 99(C5):10143–10162, 1994. doi: 10.1029/94JC00572.

G. Evensen. *Data Assimilation. The Ensemble Kalman Filter*. Springer-Verlag, New York, 2006.

M. Fazel, R. Ge, S. Kakade, and M. Mesbahi. Global Convergence of Policy Gradient Methods for the Linear Quadratic Regulator. In *International Conference on Machine Learning*, pages 1467–1476. PMLR, July 2018. URL <http://proceedings.mlr.press/v80/fazel18a.html>. ISSN: 2640-3498.

W. H. Fleming. Exit probabilities and optimal stochastic control. *Applied Mathematics and Optimization*, 4(1):329–346, 1977.

W. H. Fleming and S. K. Mitter. Optimal Control and Nonlinear Filtering for Nondegenerate Diffusion Processes. *Stochastics*, 8(1):63–77, January 1982. ISSN 0090-9491. doi: 10.1080/17442508208833228. URL <https://doi.org/10.1080/17442508208833228>.

S. Fujimoto, H. van Hoof, and D. Meger. Addressing function approximation error in actor-critic methods. In Jennifer Dy and Andreas Krause, editors, *Proceedings of the 35th International Conference on Machine Learning*, volume 80 of *Proceedings of Machine Learning Research*, pages 1587–1596. PMLR, 10–15 Jul 2018. URL <http://proceedings.mlr.press/v80/fujimoto18a.html>.

T. T. Georgiou and A. Lindquist. The separation principle in stochastic control, redux. *IEEE Transactions on Automatic Control*, 58(10):2481–2494, 2013.

C. Hartmann and C. Schütte. Efficient rare event simulation by optimal nonequilibrium forcing. *Journal of Statistical Mechanics: Theory and Experiment*, 2012(11):P11004, 2012.

P. L. Houtekamer and H. L. Mitchell. A sequential ensemble Kalman filter for atmospheric data assimilation. *Monthly Weather Review*, 129(1):123–137, 2001.

J. P. Jansch-Porto, B. Hu, and G. E. Dullerud. Convergence guarantees of policy optimization methods for Markovian jump linear systems. In *2020 American Control Conference (ACC)*, pages 2882–2887. IEEE, 2020.

R. E. Kalman. Contributions to the theory of optimal control. *Boletin de la Sociedad Matematica Mexicana* (2), 5:102–109, 1960.

H. J. Kappen and H. C. Ruiz. Adaptive importance sampling for control and inference. *Journal of Statistical Physics*, 162(5):1244–1266, 2016.

J. W. Kim and P. G. Mehta. An optimal control derivation of nonlinear smoothing equations. In *Proceedings of the Workshop on Dynamics, Optimization and Computation held in honor of the 60th birthday of Michael Dellnitz*, pages 295–311. Springer, 2020.

Peter E Kloeden and Eckhard Platen. *Numerical Solution of Stochastic Differential Equations*. Springer, Applications of Mathematics, 1999.

P. Lancaster and L. Rodman. *Algebraic Riccati Equations*. Clarendon press, 1995.

A. J. Laub. Invariant subspace methods for the numerical solution of Riccati equations. In *The Riccati Equation*, pages 163–196. Springer, 1991.

H. R. Maei, C. Szepesvári, S. Bhatnagar, and R. S. Sutton. Toward off-policy learning control with function approximation. In *Proceedings of the 27th International Conference on International Conference on Machine Learning*, ICML'10, page 719–726, Madison, WI, USA, 2010. Omnipress. ISBN 9781605589077.

D. Malik, A.n Pananjady, K. Bhatia, K. Khamaru, P. L. Bartlett, and M. J. Wainwright. Derivative-Free Methods for Policy Optimization: Guarantees for Linear Quadratic Systems. *Journal of Machine Learning Research*, 21(21):1–51, 2020. ISSN 1533-7928. URL <http://jmlr.org/papers/v21/19-198.html>.

P. G. Mehta and S. P. Meyn. Q-learning and Pontryagin’s minimum principle. In *Proceedings of the 48h IEEE Conference on Decision and Control (CDC) held jointly with 2009 28th Chinese Control Conference*, pages 3598–3605. IEEE, 2009.

F. S. Melo, S. P. Meyn, and M. I. Ribeiro. An analysis of reinforcement learning with function approximation. In *Proceedings of the 25th International Conference on Machine Learning*, ICML '08, page 664–671, New York, NY, USA, 2008. Association for Computing Machinery. ISBN 9781605582054. doi: 10.1145/1390156.1390240. URL <https://doi.org/10.1145/1390156.1390240>.

S. K. Mitter and N. J. Newton. A variational approach to nonlinear estimation. *SIAM journal on control and optimization*, 42(5):1813–1833, 2003.

H. Mohammadi, A. Zare, M. Soltanolkotabi, and M. R. Jovanovic. Global exponential convergence of gradient methods over the nonconvex landscape of the linear quadratic regulator. In *2019 IEEE 58th Conference on Decision and Control (CDC)*, pages 7474–7479, December 2019. doi: 10.1109/CDC40024.2019.9029985. ISSN: 2576-2370.

H. Mohammadi, M. R. Jovanovic, and M. Soltanolkotabi. Learning the model-free linear quadratic regulator via random search. In *Learning for Dynamics and Control*, pages 531–539. PMLR, July 2020a. URL <http://proceedings.mlr.press/v120/mohammadi20a.html>. ISSN: 2640-3498.

H. Mohammadi, M. Soltanolkotabi, and M. R. Jovanovic. Random search for learning the linear quadratic regulator. In *2020 American Control Conference (ACC)*, pages 4798–4803, July 2020b. doi: 10.23919/ACC45564.2020.9147749. ISSN: 2378-5861.

H. Mohammadi, M. Soltanolkotabi, and M. R. Jovanovic. On the Linear Convergence of Random Search for Discrete-Time LQR. *IEEE Control Systems Letters*, 5(3):989–994, July 2021. ISSN 2475-1456. doi: 10.1109/LCSYS.2020.3006256. Conference Name: IEEE Control Systems Letters.

D. Nualart and É. Pardoux. Stochastic calculus with anticipating integrands. *Probability Theory and Related Fields*, 78(4):535–581, 1988.

S. Pathiraja, S. Reich, and W. Stannat. McKean-vlasov sdes in nonlinear filtering. *arXiv preprint arXiv:2007.12658*, 2020.

K. Rawlik, M. Toussaint, and S. Vijayakumar. On stochastic optimal control and reinforcement learning by approximate inference. In *Twenty-third international joint conference on artificial intelligence*, 2013.

S. Reich and C. Cotter. *Probabilistic forecasting and Bayesian data assimilation*. Cambridge University Press, 2015.

C. Schütte, S. Winkelmann, and C. Hartmann. Optimal control of molecular dynamics using markov state models. *Mathematical programming*, 134(1):259–282, 2012.

T. Sutter, A. Ganguly, and H. Koepll. A variational approach to path estimation and parameter inference of hidden diffusion processes. *Journal of Machine Learning Research*, 17:6544–80, 2016.

A. Taghvaei and P. G. Mehta. An optimal transport formulation of the ensemble Kalman filter. *IEEE Transactions on Automatic Control*, pages 1–1, 2020. doi: 10.1109/TAC.2020.3015410.

A. Taghvaei, J. de Wiljes, P. G. Mehta, and S. Reich. Kalman filter and its modern extensions for the continuous-time nonlinear filtering problem. *Journal of Dynamic Systems, Measurement, and Control*, 140(3):030904, 2018. doi: 10.1115/1.4037780.

A. Taghvaei, P. G. Mehta, and S. P. Meyn. Diffusion map-based algorithm for gain function approximation in the feedback particle filter. *SIAM/ASA Journal on Uncertainty Quantification*, 8(3):1090–1117, 2020.

Amirhossein Taghvaei. *Design and analysis of particle-based algorithms for nonlinear filtering and sampling*. PhD thesis, University of Illinois at Urbana-Champaign, 2019.

Amirhossein Taghvaei and Prashant G Mehta. Error analysis for the linear feedback particle filter. In *2018 Annual American Control Conference (ACC)*, pages 4261–4266. IEEE, 2018. doi: 10.23919/ACC.2018.8430867.

R. Tedrake. Underactuated Robotics: Algorithms for Walking, Running, Swimming, Flying, and Manipulation (course Notes for MIT 6.832). URL <http://underactuated.mit.edu/>. Last accessed on 16 May 2021.

E. Theodorou, J. Buchli, and S. Schaal. A generalized path integral control approach to reinforcement learning. *The Journal of Machine Learning Research*, 11:3137–3181, 2010.

E. Todorov. General duality between optimal control and estimation. In *2008 47th IEEE Conference on Decision and Control*, pages 4286–4292, Dec 2008.

E. Todorov. Efficient computation of optimal actions. *Proceedings of the national academy of sciences*, 106(28):11478–11483, 2009.

S. Tu and B. Recht. The Gap Between Model-Based and Model-Free Methods on the Linear Quadratic Regulator: An Asymptotic Viewpoint. In *Conference on Learning Theory*, pages 3036–3083. PMLR, June 2019. URL <http://proceedings.mlr.press/v99/tu19a.html>. ISSN: 2640-3498.

R. Van Handel. Filtering, stability, and robustness. *PhD thesis, California Institute of Technology*, 2006.

R. Van Handel. Stochastic calculus, filtering, and stochastic control. *Course notes.*, URL <http://www.princeton.edu/rvan/acm217/ACM217.pdf>, 14, 2007.

T. Yang, P. G. Mehta, and S. P. Meyn. Feedback particle filter. *IEEE Transactions on Automatic Control*, 58(10):2465–2480, October 2013. doi: 10.1109/TAC.2013.2258825.

K. Zhang, B. Hu, and T. Basar. On the Stability and Convergence of Robust Adversarial Reinforcement Learning: A Case Study on Linear Quadratic Systems. *Advances in Neural Information Processing Systems*, 33:22056–22068, 2020. URL <https://proceedings.neurips.cc/paper/2020/hash/fb2e203234df6dee15934e448ee88971-Abstract.html>.

A Proof of Prop. 1

It is first shown that the conditional mean \bar{m}_t and the conditional covariance $\bar{\Sigma}_t$ evolve according to the Kalman filter equations (3). The SDE for the mean is obtained by taking the conditional expectation of (4),

$$d\bar{m}_t = A\bar{m}_t dt + BU_t dt + \bar{L}_t(dZ_t - H\bar{m}_t dt)$$

where we used the fact that U_t is assumed to be \mathcal{Z}_t measurable.

To obtain the equation for the covariance, define the error process $e_t = \bar{X}_t - \bar{m}_t$ which evolves according to

$$de_t = (A - \frac{1}{2}\bar{L}_t H)e_t dt + d\bar{\xi}_t$$

Then, upon an application of the Itô rule

$$d(e_t e_t^\top) = (A - \frac{1}{2}\bar{L}_t H)(e_t e_t^\top) dt + (e_t e_t^\top)(A - \frac{1}{2}\bar{L}_t H)^\top dt + Q dt + d\bar{\xi}_t e_t^\top + e_t d\bar{\xi}_t^\top$$

and taking the conditional expectation, the equation for the conditional covariance $\bar{\Sigma}_t = \mathbb{E}[e_t e_t^\top | \mathcal{Z}_t]$ is obtained as

$$\frac{d}{dt} \bar{\Sigma}_t = A \bar{\Sigma}_t + \bar{\Sigma}_t A^\top + Q - \bar{\Sigma}_t H^\top H \bar{\Sigma}_t$$

where we used the definition $\bar{L}_t = \bar{\Sigma}_t H^\top$.

The equation for the conditional covariance $\bar{\Sigma}_t$ is identical to the DRE (3b). Therefore, if the initial condition $\bar{\Sigma}_0 = \Sigma_0$ then $\bar{\Sigma}_t = \Sigma_t$ for all $t > 0$. This also implies $\bar{L}_t = L_t$, which in turn implies that the SDE for the conditional mean \bar{m}_t is identical to Kalman filter equation for m_t . If $\bar{m}_0 = m_0$ then $\bar{m}_t = m_t$ for all $t > 0$.

By replacing the mean-field terms \bar{m}_t and $\bar{\Sigma}_t$ by exogenous processes m_t and Σ_t , the McKean-Vlasov SDE (4) simplifies to an Ornstein-Uhlenbeck SDE. Because the distribution of the initial condition \bar{X}_0 is Gaussian, the distribution of \bar{X}_t is also Gaussian and given by $\mathcal{N}(m_t, \Sigma_t)$.

B Proof of Prop. 2

The proof is similar to the proof of Prop. 1. The equation for the mean \bar{n}_t is obtained by taking the expectation of SDE (8),

$$d\bar{n}_t = (A + \bar{S}_t C^\top C) \bar{n}_t dt$$

Because $\bar{n}_T = 0$, we have $\bar{n}_t = 0$ for all $t \in [0, T]$.

The equation for the covariance \bar{S}_t is obtained by writing the SDE for the error $e_t := \bar{Y}_t - \bar{n}_t$:

$$de_t = (A + \frac{1}{2} \bar{S}_t C^\top C) e_t dt + B d\bar{\eta}_t,$$

Using the Itô rule for $e_t e_t^\top$,

$$d(e_t e_t^\top) = (A + \frac{1}{2} \bar{S}_t C^\top C)(e_t e_t^\top) dt + (e_t e_t^\top)(A + \frac{1}{2} \bar{S}_t C^\top C)^\top - BR^{-1} B^\top + B d\bar{\eta}_t e_t^\top + e_t (B d\bar{\eta}_t)^\top$$

The Itô correction term appears with a negative sign because the SDE involves a backward Wiener process $\bar{\eta}_t$ [Nualart and Pardoux, 1988, Sec. 4.2]. Taking an expectation yields the following equation for \bar{S}_t :

$$\frac{d}{dt} \bar{S}_t = (A + \frac{1}{2} \bar{S}_t C^\top C) \bar{S}_t + \bar{S}_t (A + \frac{1}{2} \bar{S}_t C^\top C)^\top - BR^{-1} B^\top$$

The SDE is identical to the SDE for S_t . Because $\bar{S}_T = S_T$, we have $\bar{S}_t = S_t$ for all $t \in [0, T]$. The conclusion that \bar{Y}_t is Gaussian follows from the fact that with $\bar{n}_t = n_t$ and $\bar{S}_t = S_t$, the SDE for \bar{Y}_t is an Ornstein-Uhlenbeck SDE with a Gaussian terminal condition.

The proof for the rest of proposition is straightforward. By definition,

$$\begin{aligned} \mathbb{E}[\bar{Y}_t] &= \mathbb{E}[\bar{S}_t^{-1}(\bar{Y}_t - \bar{n}_t)] = \bar{S}_t^{-1}(\bar{n}_t - \bar{n}_t) = 0 \\ \mathbb{E}[\bar{Y}_t \bar{Y}_t^\top] &= \mathbb{E}[\bar{S}_t^{-1}(\bar{Y}_t - \bar{n}_t)(\bar{Y}_t - \bar{n}_t)^\top \bar{S}_t^{-1}] = \bar{S}_t^{-1} = S_t^{-1} = P_t \end{aligned}$$

Since $\mathbb{E}[\bar{Y}_t \bar{Y}_t^\top] = P_t$, the optimal gain matrix $K_t = -R^{-1} B^\top \mathbb{E}[\bar{Y}_t \bar{Y}_t^\top]$. For a given $x \in \mathbb{R}^d$, the optimal control $u_t(x) = K_t x = -R^{-1} B^\top \mathbb{E}[\bar{Y}_t \bar{Y}_t^\top] x$ is the unique minimizer of the Hamiltonian. This is referred to as the minimum principle of optimal control.

C Details of the algorithms to solve the partially observed LQG problem in Sec. 2

In this section, the implementation details of the EnKF-based algorithms are presented to numerically solve the partially observed LQG problem (1)-(2) introduced in the main body of the paper. For better readability, the overall algorithm is broken down into three separate algorithms:

1. Algorithm 1 is an offline algorithm. It is based on the finite- N approximation of the (control) EnKF as described in Sec. 2.2 of the main body of the paper. The algorithm is run offline to obtain an approximation of the $\{P_t : 0 \leq t \leq T\}$.

2. Algorithm 2 is an online algorithm. It is based on the finite- N approximation of the (filter) EnKF as described in Sec. 2.1 of the main body of the paper. The algorithm is run online in a real-time manner. At each time step, it processes the sensor measurements from the true system (plant) and computes the optimal control input by calling Algorithm 3.
3. Algorithm 3 computes the optimal control input. It is based upon minimization of the Hamiltonian function. In an online implementation, the optimal control input is applied to the plant at each time step.

The input structure of each of the three algorithms is clearly delineated. In particular, the algorithms require *only* the simulator in the form of the function evaluator $f(x, u) = Ax + Bu$ for the dynamics, $c(x) = Cx$ for the cost function, and $h(x) = Hx$ for the observation function. The algorithms do not require solution of the DRE.

Remark 5. *In a numerical implementation of step 1 and step 2, there are two sources of error: (i) error on account of finite- N approximation; and (ii) error on account of time discretization which depends upon the step size Δt . The finite- N approximation error has been studied in the EnKF literature where it is shown that the error in approximating $\|P_t - P_t^{(N)}\|$ (in step 1) and the error in approximating the gain the mean $\|\hat{X}_t - \hat{X}_t^{(N)}\|$ (in step 2) converges to zero with the rate $O(\frac{1}{\sqrt{N}})$ Del Moral and Tugaut [2018], Bishop et al. [2019], Bishop and Del Moral [2018], Taghvaei and Mehta [2018], Taghvaei [2019]. The time discretization error is also expected to be bounded and converges to zero with the rate $O(\Delta t)$ when the system is stable Kloeden and Platen [1999].*

Algorithm 1 [offline] EnKF algorithm to approximate $\{P_t : 0 \leq t \leq T\}$

Input: Simulation time T , simulation step-size Δt , number of particles N , simulator $f(x, u) = Ax + Bu$, terminal cost P_T , cost function $c(x) = Cx$, and control cost matrix R .

Output: $\{P_k^{(N)} : k = 0, 1, 2, \dots, \frac{T}{\Delta t}\}$.

- 1: $T_F = \frac{T}{\Delta t}$
- 2: $P_{T_F}^{(N)} = P_T$
- 3: Initialize $\{\mathcal{Y}_{T_F}^i\}_{i=1}^N \stackrel{\text{i.i.d}}{\sim} \mathcal{N}(0, P_T^{-1})$
- 4: calculate $n_{T_F}^{(N)} = N^{-1} \sum_{i=1}^N \mathcal{Y}_{T_F}^i$
- 5: **for** $k = T_F$ to 1 **do**
- 6: Calculate $\hat{c}_k^{(N)} = N^{-1} \sum_{i=1}^N c(\mathcal{Y}_k^i)$
- 7: Calculate $M_k^{(N)} = (N - 1)^{-1} \sum_{i=1}^N (\mathcal{Y}_k^i - n_k^{(N)})(c(\mathcal{Y}_k^i) - \hat{c}_k^{(N)})^\top$
- 8: **for** $i = 1 : N$ **do**
- 9: $\Delta \eta_k^i \stackrel{\text{i.i.d}}{\sim} \mathcal{N}(0, \frac{1}{\Delta t} R^{-1})$
- 10: $\Delta \mathcal{Y}_k^i = f(\mathcal{Y}_k^i, \Delta \eta_k^i) \Delta t + \frac{1}{2} M_k^{(N)} (c(\mathcal{Y}_k^i) + \hat{c}_k^{(N)}) \Delta t$
- 11: $\mathcal{Y}_{k-1}^i = \mathcal{Y}_k^i - \Delta \mathcal{Y}_k^i$
- 12: **end for**
- 13: Calculate $n_{k-1}^{(N)} = N^{-1} \sum_{i=1}^N \mathcal{Y}_{k-1}^i$
- 14: Calculate $S_{k-1}^{(N)} = (N - 1)^{-1} \sum_{i=1}^N (\mathcal{Y}_{k-1}^i - n_{k-1}^{(N)})(\mathcal{Y}_{k-1}^i - n_{k-1}^{(N)})^\top$
- 15: $P_{k-1}^{(N)} = (S_{k-1}^{(N)})^{-1}$
- 16: **end for**

Algorithm 2 [online] EnKF algorithm to approximate state estimate \hat{X}_t and optimal control u_t

Input: Simulation time T , simulation step-size Δt , number of particles N , simulator $f(x, u) = Ax + Bu$, initial distribution $\mathcal{N}(m_0, \Sigma_0)$, process noise covariance \mathcal{R} , observation function $h(x) = Hx$, $\{P_k^{(N)} : k = 0, 1, 2, \dots, \frac{T}{\Delta t}\}$ from the offline algorithm 1.

Output: estimate $\{\hat{X}_k^{(N)} : k = 0, 1, 2, \dots, \frac{T}{\Delta t}\}$ and optimal control input $\{u_k^{(N)} : k = 0, 1, 2, \dots, \frac{T}{\Delta t} - 1\}$.

- 1: Define $T_F := \frac{T}{\Delta t}$
- 2: Initialize particles $\{X_0^i\}_{i=1}^N \stackrel{\text{i.i.d.}}{\sim} \mathcal{N}(m_0, \Sigma_0)$
- 3: **for** $k = 0$ to $T_F - 1$ **do**
- 4: Calculate $\hat{X}_k^{(N)} = \frac{1}{N} \sum_{i=1}^N X_k^i$
- 5: Calculate $u_k^{(N)} = \arg \min_a \mathcal{H}(\hat{X}_k^{(N)}, P_k^{(N)} \hat{X}_k^{(N)}, a)$ from algorithm 3
- 6: Apply control $u_k^{(N)}$ to the true system and obtain the observation $\Delta Z_k = Z_{(k+1)\Delta t} - Z_{k\Delta t}$
- 7: Calculate $\hat{h}_k^{(N)} = \frac{1}{N} \sum_{i=1}^N h(X_k^i)$
- 8: Calculate $L_k^{(N)} = \frac{1}{N-1} \sum_{i=1}^N (X_k^i - \hat{X}_k^{(N)})(h(X_k^i) - \hat{h}_k^{(N)})^\top \mathcal{R}^{-1}$
- 9: **for** $i = 1$ to N **do**
- 10: $\Delta \xi_k^i \stackrel{\text{i.i.d.}}{\sim} \mathcal{N}(0, Q\Delta t)$
- 11: $\Delta X_k^i = f(X_k^i, u_k^{(N)})\Delta t + \Delta \xi_k^i + L_k^{(N)}(\Delta Z_k - \frac{h(X_k^i) + \hat{h}_k^{(N)}}{2}\Delta t)$
- 12: $X_{k+1}^i = X_k^i + \Delta X_k^i$
- 13: **end for**
- 14: **end for**

Algorithm 3 Computation of optimal control

Input: state x , momentum y , control cost matrix R ,
Hamiltonian $\mathcal{H}(x, y, \alpha) = y^\top (a(x) + b(x)\alpha) + \frac{1}{2}|c(x)|^2 + \frac{1}{2}\alpha^\top R\alpha$.

Output: optimal control $u = \arg \min_\alpha \mathcal{H}(x, y, \alpha)$.

- 1: **if** $b(x)$ is known **then**
- 2: $u = -R^{-1}b(x)^\top y$
- 3: **else**
- 4: **for** $k = 1$ to m **do**
- 5: $e_k = [0, \dots, 0, \underbrace{1}_{k\text{-th component}}, 0, \dots, 0] \in \mathbb{R}^m$
- 6: $u_k = \mathcal{H}(x, y, R^{-1}e_k) - \mathcal{H}(x, y, 0) - \frac{1}{2}(R^{-1})_{kk}$
- 7: **end for**
- 8: **end if**

D Proof of the Prop. 3

The probability density $p_t(x) \propto e^{-v_t(x)}$ (by definition). We begin by deriving the evolution equation (14) for p_t . Write $v_t = -\log(p_t) + \beta_t$ where β_t is a time-dependent constant to ensure p_t is normalized. In terms of p_t and β_t , the HJB equation (12) for v_t is written as

$$-\frac{1}{p_t} \frac{\partial p_t}{\partial t} + \dot{\beta}_t + \frac{1}{2}|c|^2 - \frac{1}{p} a^\top \nabla p - \frac{1}{2} \frac{1}{p_t} \text{Tr}(D \nabla^2 p_t) - \frac{1}{2} \text{Tr}((Q - D) \nabla^2 \log(p_t)) = 0$$

where we used $\nabla^2 \log(p_t) = \frac{1}{p_t} \nabla^2 p_t - \frac{1}{p_t^2} \nabla p_t \nabla p_t^\top$. Multiplying by p_t yields

$$\frac{\partial p_t}{\partial t} = (h_t + \dot{\beta}_t)p_t - \nabla \cdot (p_t a) + \nabla \cdot (p_t \nabla \cdot D) - \frac{1}{2} \nabla^2 \cdot (p_t D)$$

where we used

$$h_t := \frac{1}{2}|c|^2 + \nabla \cdot a - \frac{1}{2} \nabla^2 \cdot D + \frac{1}{2} \text{Tr}((D - Q) \nabla^2 \log(p_t))$$

$$a^\top \nabla p_t = \nabla \cdot (p_t a) - p_t \nabla \cdot a$$

$$\text{Tr}(D \nabla^2 p_t) = \nabla^2 \cdot (p_t D) - 2 \nabla \cdot (p_t \nabla \cdot D) + p_t \nabla^2 \cdot D$$

Noting $\int \frac{\partial p_t}{\partial t} dx = 0$, we obtain

$$\dot{\beta} = - \int h_t(x) p_t(x) dx = -\hat{h}_t$$

which in turn gives the PDE (14) for p_t .

The proof for $\bar{p}_t = p_t$ follows from showing that the evolution equation for \bar{p}_t and p_t are identical. Consider the SDE (15). The evolution equation for the density \bar{p}_t is the Fokker-Planck equation:

$$\frac{\partial \bar{p}_t}{\partial t} = -\nabla \cdot (\bar{p}_t a) - \nabla \cdot (\bar{p}_t \nabla \cdot D) - \nabla \cdot (\bar{p}_t \mathcal{V}_t) - \frac{1}{2} \nabla^2 \cdot (\bar{p}_t D)$$

where the diffusion term $\frac{1}{2} \nabla^2 \cdot (\bar{p}_t D)$ appears with a negative sign because $\bar{\eta}_t$ is a backward Wiener process.

It is easily see that if the vector-field $\mathcal{V}_t(\cdot)$ solves the PDE (16) then the evolution equations for p_t and \bar{p}_t are identical.

E Finite- N algorithm to solve the nonlinear optimal control problem in Sec. 3

This is continuation of Remark 3 in the main body of the paper. In particular, we assume two approximations: (i) $h_t(x) \approx \frac{1}{2}|c(x)|^2$ and (ii) \bar{p}_t is a Gaussian density.

The finite- N algorithm involves simulating a system of interacting particles $\{\mathcal{Y}_t^i \in \mathbb{R}^d : 0 \leq t \leq T, i = 1, \dots, N\}$ according to

$$d\mathcal{Y}_t^i = a(\mathcal{Y}_t^i) dt + b(\mathcal{Y}_t^i) d\bar{\eta}_t^i + M_t^{(N)} \left(\frac{c(\mathcal{Y}_t^i) + \hat{c}_t^{(N)}}{2} \right) dt, \quad \mathcal{Y}_T^i \stackrel{\text{i.i.d.}}{\sim} e^{-g_T}$$

where $\hat{c}_t^{(N)} := N^{-1} \sum_{i=1}^N c(\bar{\mathcal{Y}}_t^i)$, $\eta^i := \{\eta_t^i \in \mathbb{R}^m : i : 0 \leq t \leq T\}$ is an independent copy of $\bar{\eta}$ and the control gain

$$M_t^{(N)} = \frac{1}{N-1} \sum_{i=1}^N (\mathcal{Y}_t^i - n_t^{(N)}) (c(\mathcal{Y}_t^i) - \hat{c}_t^{(N)})^\top$$

where $n_t^{(N)} := \frac{1}{N} \sum_{i=1}^N \mathcal{Y}_t^i$.

To obtain the control, compute the empirical covariance

$$S_t^{(N)} = \frac{1}{N-1} \sum_{i=1}^N (\mathcal{Y}_t^i - n_t^{(N)}) (\mathcal{Y}_t^i - n_t^{(N)})^\top$$

and use it to define

$$Y_t^i = (S_t^{(N)})^{-1} (\mathcal{Y}_t^i - n_t^{(N)})$$

If the function $b(x)$ is known, the approximate formula for the optimal control is obtained as

$$u_t(x) = -\frac{1}{N-1} \sum_{i=1}^N R^{-1} (b(x)^\top Y_t^i) (Y_t^i)^\top x$$

This step is justified using the Gaussian approximation of the density.

If the function $b(x)$ is not known, the optimal control input is evaluated by minimizing the Hamiltonian. The overall algorithm is described in algorithm 4.

Algorithm 4 EnKF algorithm to approximate the optimal control law for the nonlinear problem.

Input: Simulation time T , simulation step-size Δt , number of particles N , simulator $f(x, u) = a(x) + b(x)u$, terminal cost g_T , cost function $c(x)$, and control cost matrix R .

Output: optimal control law $\{u_k^{(N)}(x) : k = 0, 1, 2, \dots, \frac{T}{\Delta t} - 1\}$

- 1: $T_F = \frac{T}{\Delta t}$
- 2: Initialize $\{\mathcal{Y}_{T_F}^i\}_{i=1}^N \stackrel{\text{i.i.d.}}{\sim} e^{-g_T}$
- 3: calculate $n_{T_F}^{(N)} = N^{-1} \sum_{i=1}^N \mathcal{Y}_{T_F}^i$
- 4: **for** $k = T_F$ to 1 **do**
- 5: Calculate $\hat{c}_k^{(N)} = N^{-1} \sum_{i=1}^N c(\mathcal{Y}_k^i)$
- 6: Calculate $M_k^{(N)} = (N - 1)^{-1} \sum_{i=1}^N (\mathcal{Y}_k^i - n_k^{(N)})(c(\mathcal{Y}_k^i) - \hat{c}_k^{(N)})^\top$
- 7: **for** $i = 1$ to N **do**
- 8: $\Delta \eta_k^i \stackrel{\text{i.i.d.}}{\sim} \mathcal{N}(0, \frac{1}{\Delta t} R^{-1})$
- 9: $\Delta \mathcal{Y}_k^i = f(\mathcal{Y}_k^i, \Delta \eta_k^i) \Delta t + \frac{1}{2} M_k^{(N)} (c(\mathcal{Y}_k^i) + \hat{c}_k^{(N)}) \Delta t$
- 10: $\mathcal{Y}_{k-1}^i = \mathcal{Y}_k^i - \Delta \mathcal{Y}_k^i$
- 11: **end for**
- 12: Calculate $n_{k-1}^{(N)} = N^{-1} \sum_{i=1}^N \mathcal{Y}_{k-1}^i$
- 13: Calculate $S_{k-1}^{(N)} = (N - 1)^{-1} \sum_{i=1}^N (\mathcal{Y}_{k-1}^i - n_{k-1}^{(N)})(\mathcal{Y}_{k-1}^i - n_{k-1}^{(N)})^\top$
- 14: $P_{k-1}^{(N)} = (S_{k-1}^{(N)})^{-1}$
- 15: compute $u_{k-1}^{(N)}(x) = \arg \min_{\alpha} \mathcal{H}(x, P_{k-1}^{(N)} x, \alpha)$ from algorithm 3
- 16: **end for**

F Details of the numerical examples in Sec. 4

Notation: $\mathcal{I}_n \in \mathbb{R}^{n \times n}$ denotes the identity matrix.

F.1 Coupled mass spring damper system

This system is taken from Mohammadi et al. [2019]. The matrices A and B are as follows:

$$A = \begin{bmatrix} 0_{d_s \times d_s} & \mathcal{I}_{d_s} \\ -\mathbb{T} & -\mathbb{T} \end{bmatrix}, \quad B = \begin{bmatrix} 0_{d_s \times d_s} \\ \mathcal{I}_{d_s} \end{bmatrix}$$

where $d_s = \frac{d}{2}$ is the number of masses and $\mathbb{T} \in \mathbb{R}^{d_s \times d_s}$ is a Toeplitz matrix with 2 on the main diagonal and -1 on the first sub-diagonal and first super-diagonal. Additional model and simulation parameters are listed in Table 1 and 2, respectively.

Table 1: Model parameters for the coupled mass spring damper system

Model parameter	Numerical value
m_0	$0_{d \times 1}$
Σ_0	$0.1 \mathcal{I}_d$
C for $d = 2$	$\sqrt{5} \mathcal{I}_d$
C for $d = 4, 20, 50, 80$	\mathcal{I}_d
R	\mathcal{I}_{d_s}
P_T	\mathcal{I}_d
C	\mathcal{I}_d

Table 2: Simulation parameters for the coupled mass spring damper system

Simulation parameter name	Symbol	Numerical value
Simulation time	T	10
Step size for $d = 2, 4$	Δt	0.002
Step size for $d = 20, 50, 80$	Δt	0.02

F.2 Cart-pole system

The nonlinear model is taken from [Tedrake, Chapter 3.2.1]:

$$\begin{aligned}\dot{\theta} &= \omega \\ \dot{\omega} &= \frac{1}{l(M+m\sin^2(\theta))} (-F\cos(\theta) - ml\omega^2\cos(\theta)\sin(\theta) - (m+M)g\sin(\theta)) \\ \dot{x} &= v \\ \dot{v} &= \frac{1}{M+m\sin^2(\theta)} (F + m\sin(\theta)(l\omega^2 + g\cos(\theta)))\end{aligned}$$

For the LQG control design, we linearize the equations about the desired inverted equilibrium $(\pi, 0, 0, 0)$. The associated A and B matrices are as follows:

$$A = \begin{bmatrix} 0 & 0 & 1 & 0 \\ 0 & 0 & 0 & 1 \\ \frac{(M+m)g}{Ml} & 0 & 0 & 0 \\ \frac{mg}{M} & 0 & 0 & 0 \end{bmatrix}, \quad B = \begin{bmatrix} 0 \\ \frac{1}{Ml} \\ 0 \\ \frac{1}{M} \end{bmatrix}$$

The model parameters are listed in Table 3 and the simulation parameters are in Table 4.

Table 3: Model parameters for the cart-pole system

Model parameter name	Symbol	Numerical value
Mass of ball	m	0.08
Mass of cart	M	1
Length of rod	l	0.7
Gravity	g	9.81
Unstable equilibrium	$(\bar{\theta}, \bar{x}, \bar{\omega}, \bar{v})$	$(\pi, 0, 0, 0)$
Initial condition	$(\theta(0), x(0), \omega(0), v(0))$	$(1.25\pi, -0.1, 0, 0)$
	C	$\text{diag}([10, 10, 1, 1])$
LQG parameters	R	10
	P_T	\mathcal{I}_4

Table 4: Simulation parameters for the cart-pole system

Simulation parameter name	Symbol	Numerical value
Simulation time	T	10
Step size	Δt	0.0002